Journal of Sound and Vibration (2000) **231**(3), 753–764
doi:10.1006/jsvi.1999.2560, available online at http://www.idealibrary.com on IDEAL®

ACOUSTIC OPTIMIZATION OF RAILWAY SLEEPERS

J. C. O. NIELSEN

CHARMEC, Department of Solid Mechanics, Chalmers University of Technology, SE-412 96 Gothenburg, Sweden

(*Received in final form* 23 *September* 1999)

A mathematical model of vertical wheelset/track interaction is developed and adopted for minimization of sound power generated by railway sleepers (mono-bloc or bi-bloc). The influence of sleeper material properties, sleeper shape and properties of ballast and rail pads on sleeper sound power can be investigated. The wheelset/track interaction is simulated in the frequency domain by using a so-called moving irregularity model with a given displacement amplitude spectrum. Boundary element models of the acoustic medium (air) are developed for mono-bloc and bi-bloc sleepers. Radiation efficiencies are calculated and compared for the different sleeper designs. From the results obtained in a parametric study, it is concluded that the sound power generated by the sleepers is strongly influenced by ballast stiffness and damping and by rail pad stiffness. Further, it is concluded that a bi-bloc sleeper with appropriate dimensions of the connecting bar can lead to a 2–3 dB(A) reduction of sound power compared to a reference mono-bloc sleeper.

1. INTRODUCTION

Rolling noise from railway infrastructure is generally dominated by contributions from the rails. Although sound power at low frequencies (say below 500 Hz) can be dominated by sleeper radiation, the contribution from sleeper noise to the A-weighted sound power level can often be neglected. Thus, most solutions to reduce infrastructure noise focus on shape optimization and vibration attenuation of the rails. However, one possible measure to increase rail decay rates and to reduce rail noise is to increase rail pad stiffness. An increase of pad stiffness will raise sleeper vibration amplitudes and move the frequency range so that sleeper radiation is dominant towards higher frequencies [1]. As a consequence, bringing down sleeper noise becomes more important in an overall optimization of the track.

Few references on the optimization of railway track components with respect to noise radiation have been found in the literature. However, in the theoretical optimization of track components conducted by Vincent *et al.* [2], it is concluded that sound power generated by sleepers is minimized by (1) reducing rail pad stiffness, (2) increasing sleeper mass and (3) reducing the area of the upper side of the sleeper. TWINS (Track/Wheel Interaction Noise Software) [3, 4] is a tool used by

0022-460X/00/130753 + 12 $35.00/0

several European railway administrations and research institutes to study the influence of the design of wheels and track components on rolling noise.

The objective of the present study is to investigate the possibilities of designing a low-noise concrete sleeper (mono-bloc or bi-bloc). For this purpose, a mathematical model is adopted for the minimization of sound power generated by railway sleepers at frequencies below 1 kHz. Boundary element models of the acoustic medium (air) are also developed for mono-bloc and bi-bloc sleepers. Radiation efficiencies are calculated and compared for the different sleeper designs.

2. VERTICAL WHEELSET/TRACK INTERACTION MODEL

A mathematical model has been developed for the minimization of sound power generated by railway sleepers. The theory of the model is described in detail in reference [5]. The track is modelled as being geometrically repetitive and discretely supported with all sleeper bays being identical with respect to rail, rail pads, sleepers and ballast. In other words, the track is built up by an infinite number of identical linear substructures, where each substructure is a finite element model of one sleeper bay only. Steady state harmonic vibration in the frequency domain is assumed. Frequency-dependent dynamic stiffness elements at the boundaries of the model account for the infinite extension of the track. They are established by use of difference equations and are connected to the two ends of one substructure. The track model is illustrated in Figures 1 and 2.

The track is assumed to be symmetric with respect to the centre of the sleeper (xz-plane). Therefore, symmetric and antisymmetric track vibrations can be treated separately. The substructure consists of (1) one-half sleeper supported by ballast, (2) one rail with length equal to the sleeper distance and (3) one rail pad. Reference

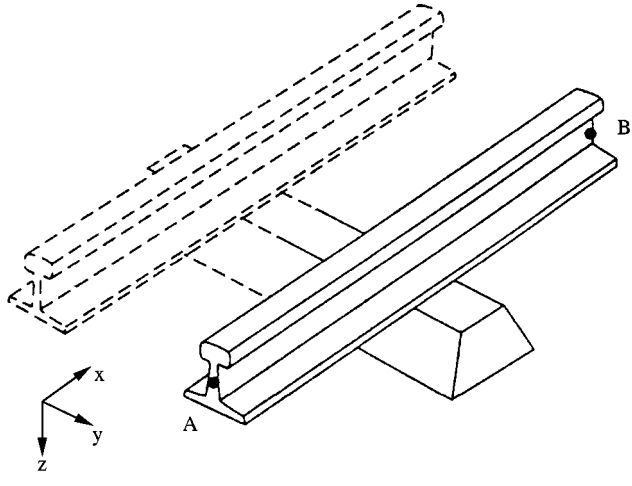

Figure 1. Illustration of one substructure in the track model. The substructure is symmetric with respect to an xz-plane between the two rails and with respect to a yz-plane cutting through the sleeper. Retained parts of the model are drawn with solid lines. Conditions accounting for an infinite track are applied at positions A and B.

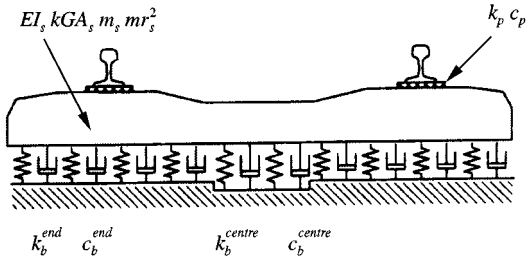

Figure 2. Mathematical model of railway track. Rail and sleeper are modelled by use of linear finite beam elements. Ballast and rail pad are hysteretically or viscously damped. Each sleeper element can be attributed different ballast properties.

data [6] from the Brite/EuRam III Silent Track project are used as input for the track model.

Rail and sleeper are modelled by use of Rayleigh–Timoshenko finite beam elements accounting for shear deformation and rotatory inertia. Each sleeper element is supported by a hysteretically or viscously damped Winkler foundation with uniform bed modulus underneath the base of the sleeper. The bed modulus can vary from one sleeper element to the next, but this option has not been adopted here. However, as indicated by measurements [7], the bed modulus is assumed to increase linearly by a factor of 10 in the frequency range 0·1–1 kHz. A discrete spring and a hysteretic or viscous damper in parallel model the rail pad.

The vertical dynamic receptance of a free–free wheelset at the nominal wheel/rail contact point is calculated by use of a three-dimensional solid finite element model. In the wheelset/track interaction model, the wheelset is treated as a dynamic substructure with the vertical displacement of the wheel/rail contact point as the only retained degree of freedom. The wheelset is coupled to the track through a spring having a linearized Hertzian contact stiffness.

Wheelset/track interaction in the frequency domain is simulated by use of a so-called moving irregularity model [8]. This means that the wheelset model is kept in a fixed chosen position along the track, and an imaginary strip containing the irregularities (roughness) on the running surfaces of wheel and rail is pulled at a steady speed at the contact point between wheelset and track. The moving irregularity is determined by a given displacement amplitude spectrum versus wavelength of the irregularities. For a given train speed this leads to a given frequency-dependent relative-displacement excitation between wheelset and track.

The roughness spectrum adopted is the sum of the vertical irregularities on wheel tread and railhead. The roughness is defined according to Silent Track reference roughness data [9]. A contact filter has been applied which accounts for the finite size of the wheel/rail contact patch. Two different roughness spectra have been investigated corresponding to a disc-braked and a block-braked wheelset, respectively.

3. REFERENCE SLEEPER

The reference sleeper is a mono-bloc prestressed concrete sleeper designed by Abetong Teknik AB in Sweden. The length and weight of the sleeper is 2·5 m and

250 kg, respectively. In the mathematical model, one-half sleeper is modelled by use of 10 linear Rayleigh–Timoshenko finite beam elements. The properties of each sleeper element are given by the bending stiffness EI, the shear stiffness kGA, the mass m per unit beam length, and the rotatory inertia mr^2 per unit beam length (see Figure 2). The properties are chosen to account for the varying cross-sectional area along the sleeper. The mathematical sleeper model has been verified successfully by use of experimental modal analysis [10]. Further, a UIC60 rail and studded 10 mm rail pads from Pandrol are adopted in the model. Track and wheelset input data are listed in references [6, 11].

4. FINITE ELEMENT ANALYSIS—REFERENCE SOUND POWER

The sound power generated by one sleeper (two halves) is calculated using the mathematical model described in Section 2 and in reference [5]. The wheelset model is held at a fixed position along the track directly above the investigated sleeper (moving irregularity model). The sleeper reference sound power W_{ref} (W) is calculated here according to

$$W_{\text{ref}}(f) = \rho_{\text{air}} c_{\text{air}} A^{\text{proj}} v^2_{\text{r.m.s.}} \tag{1}$$

where the density of air $\rho_{\text{air}} = 1{\cdot}2\ \text{kg/m}^3$ and the speed of sound $c_{\text{air}} = 340$ m/s and where A^{proj} is the projected area of the sleeper base as seen from above. The surface-averaged r.m.s. of the sleeper normal velocity is determined by

$$v_{\text{r.m.s.}}(f) = \sqrt{\frac{1}{A^{\text{proj}}} \sum_{j=1}^{N_{\text{sleeper}}} |\underline{v}(x_j, f)|^2 \, \Delta A_j^{\text{proj}}}. \tag{2}$$

Here $|\underline{v}(x_j, f)|$ is the amplitude of the complex-valued normal velocity calculated at the finite element nodes (positions x_j) of the sleeper, and ΔA_j^{proj} is the projected area of the corresponding finite elements.

The projected area of the sleeper base is adopted since the shielding properties of the ballast that may partly cover the sleeper are not known. The radiation efficiency σ of an *in situ* sleeper has been calculated by use of boundary elements analysis (see below). The active output power radiated by one sleeper is then obtained as $W_o = \sigma W_{\text{ref}}$.

4.1. SYMMETRIC TRACK VIBRATION

For symmetric track vibration, the calculated direct receptance (displacement over wheel/rail contact force) of the rail directly above a sleeper is shown in Figure 3. For the adopted track and wheelset properties [6, 11], two resonances and one antiresonance can be identified in the frequency interval investigated:

1. Resonance at 110 Hz where rail and sleepers are essentially vibrating in phase on the ballast.

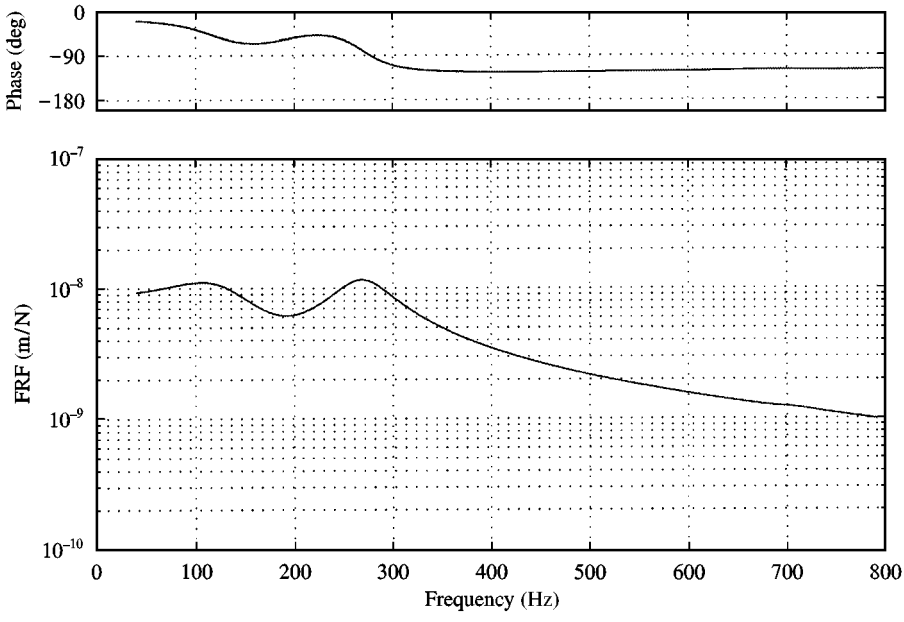

Figure 3. Calculated direct receptance/flexibility (displacement over wheel/rail contact force (m/N) of rail directly above a sleeper versus frequency. Symmetric track vibration. Input data: reference track without static preload [6]. Constant ballast stiffness.

2. Resonance at 260 Hz with a large relative motion between rail and sleepers.
3. Antiresonance at 190 Hz where the sleepers act as vibration absorbers to the rail.

The calculated wheel/rail contact force is shown in Figure 4. Note that peaks in the contact force are obtained at the so-called P2 resonance at 60 Hz (wheelset, rail and sleepers are essentially vibrating in phase on the ballast) and at the rail antiresonance at 190 Hz. The reference sound power calculated according to equations (1) and (2) for the single sleeper located directly below the position of the vehicle is shown in Figure 5. Again, three peaks can be identified:

1. P2 resonance at 60 Hz.
2. Rail antiresonance at 190 Hz.
3. Second symmetric sleeper bending eigenfrequency at 700 Hz.

The modal load of the first bending eigenmode is low since the nodes of this eigenmode are located close to the railseats. A surface plot illustrating the reference sound power calculated separately for each finite element of the sleeper located directly below the wheelset is shown in Figure 6. From this figure, the parts of the mono-bloc sleeper which give the highest contribution to the total sound power can be identified. Note that at the P2 resonance and at the antiresonance, the sleeper is essentially vibrating as a rigid body. Thus, near these frequencies, all parts of the sleeper contribute with nearly the same amount of sound power. At the second symmetric sleeper bending eigenmode, high contributions are obtained from the railseat area and the centre section of the sleeper.

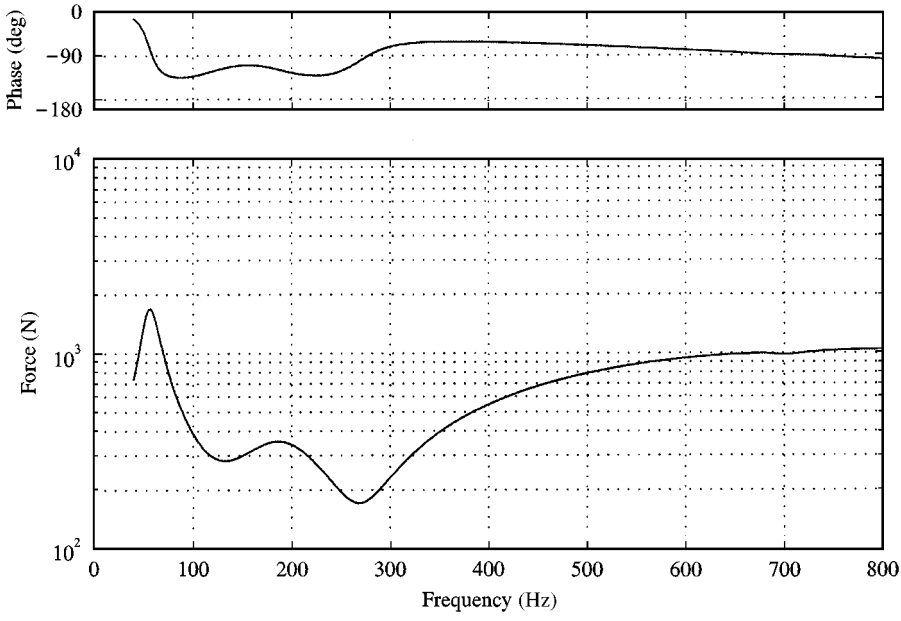

Figure 4. Calculated wheel/rail contact force (N) versus frequency. Symmetric track vibration. Input data: reference track without static preload [6]. Constant ballast stiffness.

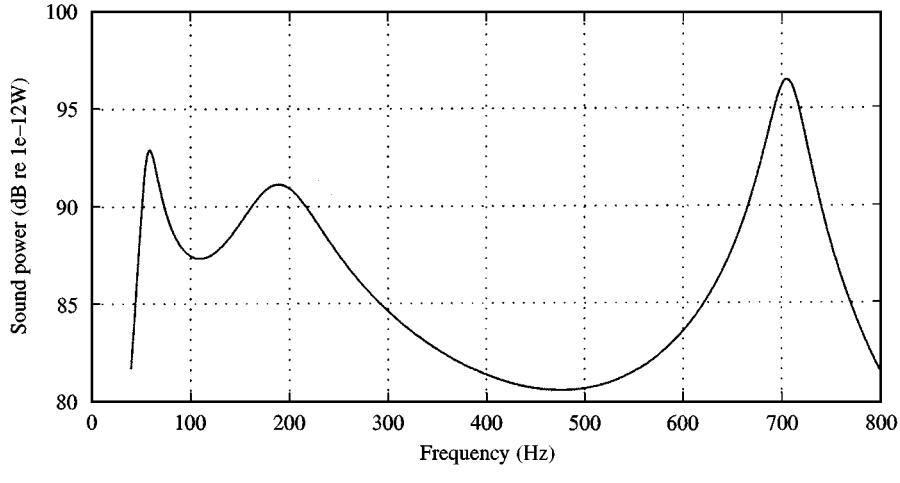

Figure 5. Reference sound power level (dB re le-12 W), calculated for the full mono-bloc sleeper (two halves) located directly below position of wheelset, versus frequency. Symmetric track vibration. Input data: reference track without static preload [6]. Constant ballast stiffness.

4.2. ANTISYMMETRIC TRACK VIBRATION

For antisymmetric track vibration, the responses are very similar to the ones shown in Figures 3–5. However, the first antisymmetric sleeper bending eigenmode can be identified at 400 Hz. In the surface plot in Figure 7, it is clear that large

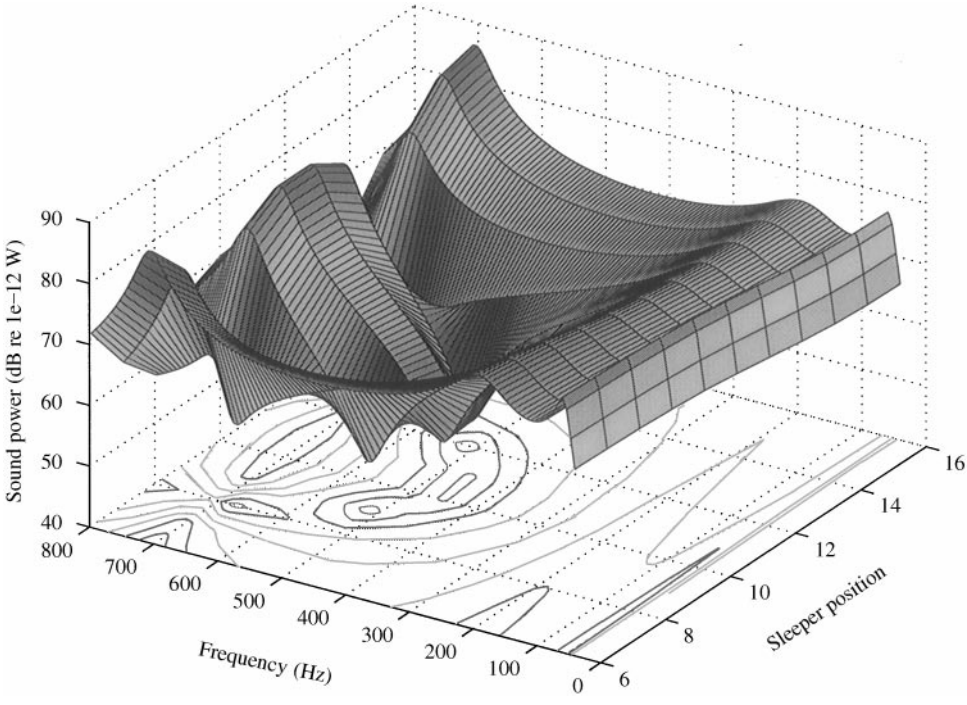

Figure 6. Reference sound power level (dB re le-12 W), calculated for each finite element of the mono-bloc half-sleeper located directly below position of vehicle, versus frequency and versus position along sleeper. Symmetric track vibration. Input data: reference track without static preload [6]. Constant ballast stiffness. Sleeper position 6 is at the sleeper end, position 10 is at the railseat and position 16 is at the sleeper centre.

sound contributions come from the sleeper ends, and (for the bending mode) also from the section between railseat and sleeper centre. Note that for antisymmetric track vibration, by definition, the velocity at sleeper centre is zero.

5. BOUNDARY ELEMENT ANALYSIS—RADIATION EFFICIENCY

In the previous section, vibration amplitudes of surface-averaged sleeper velocities were adopted to calculate sleeper reference sound power. As a rough investigation to determine how the shape of the sleeper (mono-bloc or bi-bloc) affects radiation efficiency, the sleeper optimization study is complemented with boundary element simulations by use of the commercial software SYSNOISE [12].

Boundary element models of the acoustic medium (air) developed for a single mono-bloc and bi-bloc sleeper are illustrated in Figure 8. Radiation efficiency is calculated by use of two different SYSNOISE solution methods: "collocation" and "variational". For the collocation method, a two-dimensional model of the sleeper bottom surface is built into an infinite rigid baffle. For the variational method, the three-dimensional shape of the sleeper is described in detail and a rigid plane $1{\cdot}5\ \text{m} \times 1{\cdot}5\ \text{m}$ is adopted to model the ground. Vibration velocity fields on the sleeper surface are calculated by use of three-dimensional solid finite element

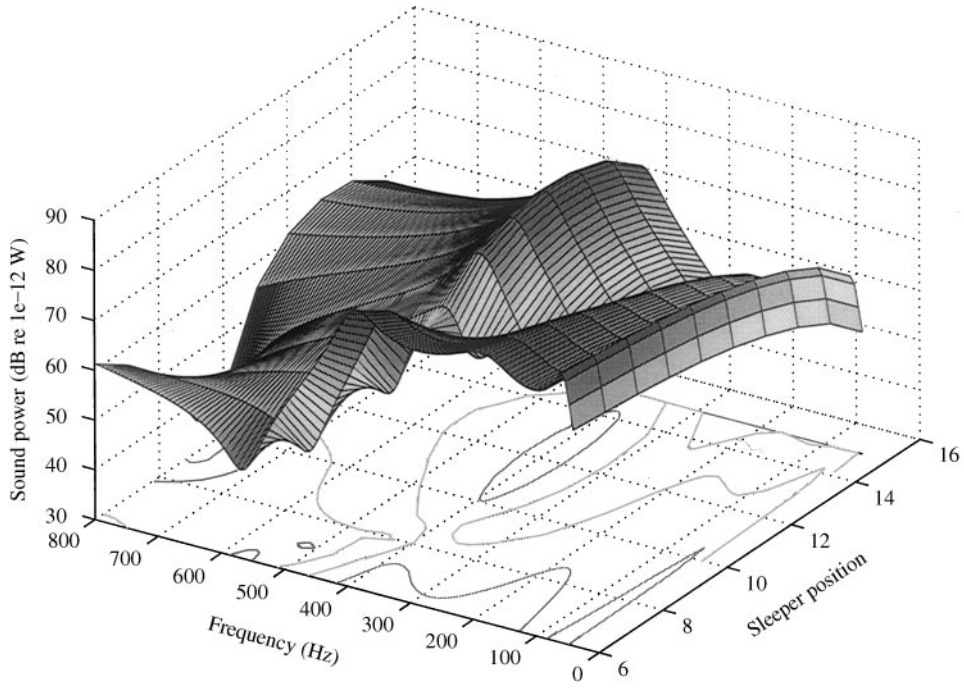

Figure 7. Reference sound power level (dB re le-12 W), calculated for each finite element of the mono-bloc half-sleeper located directly below position of vehicle, versus frequency and versus position along sleeper. Antisymmetric track vibration. Input data: reference track without static preload [6]. Constant ballast stiffness. Sleeper position 6 is at the sleeper end, position 10 is at the railseat and position 16 is at the sleeper centre.

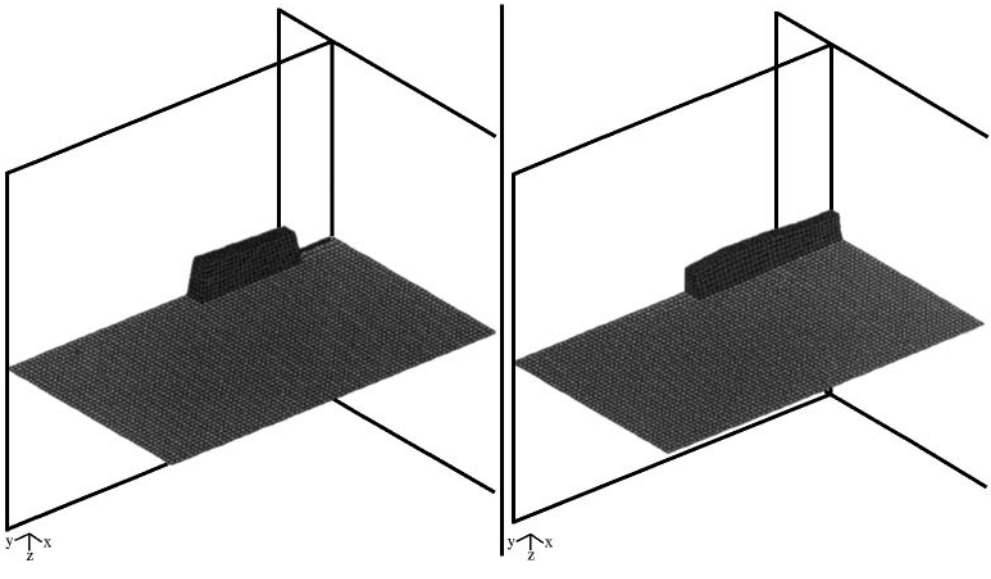

Figure 8. Illustration of boundary element models for comparison of bi-bloc and mono-bloc sleeper designs. Ground is modelled as a rigid plane 1·5 m × 1·5 m. Symmetry planes are indicated.

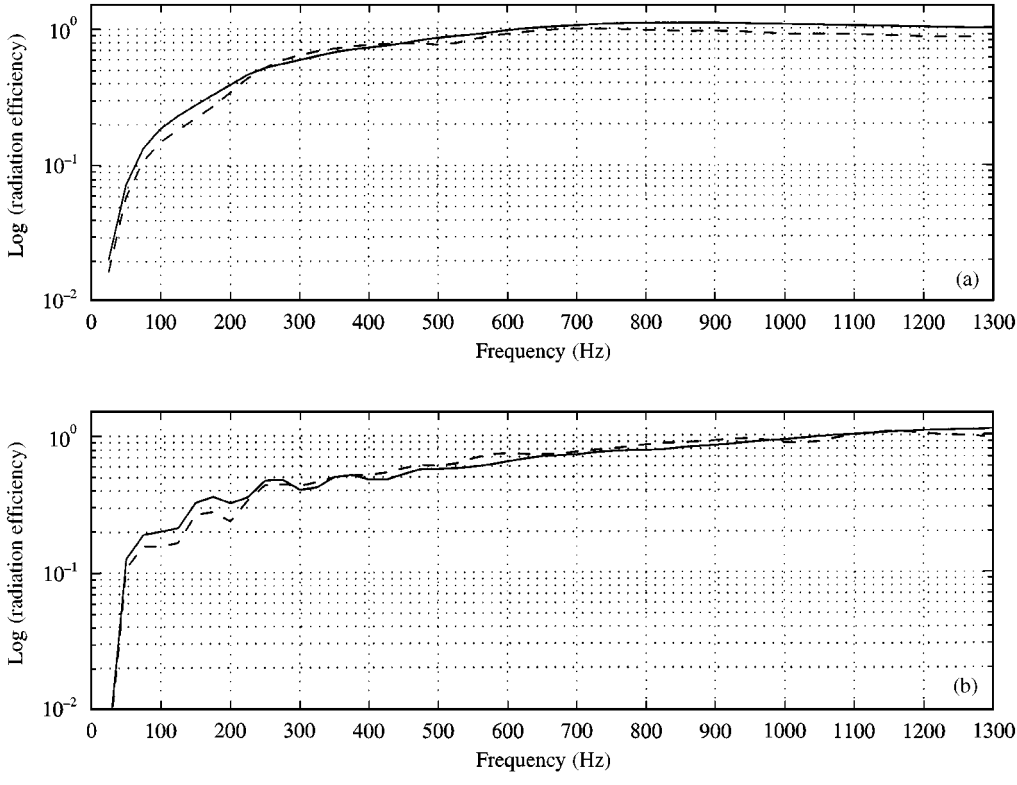

Figure 9. Calculated radiation efficiencies for single mono-bloc and bi-bloc sleeper. Sleeper is built into (a) infinite rigid baffle or (b) rigid plane 1·5 m × 1·5 m. Forced symmetric sleeper excitation at railseat. ——, mono-bloc; – – –, bi-bloc.

models and used as boundary conditions to the acoustic analyses. The only parameter that is varied between the two analyses is the sleeper shape (mono-bloc or bi-bloc). For the case of forced symmetric sleeper excitation at the railseat, a comparison between calculated radiation efficiencies for the two sleeper types and the two solution methods is shown in Figure 9. It can be seen that the shape of the sleeper seems to have a negligible influence on the radiation efficiency.

6. SLEEPER SHAPE OPTIMIZATION

The influence of several track parameters on sleeper reference sound power has been investigated for frequencies below 1 kHz [11] by use of the model described in Section 2. The parameters investigated include sleeper material properties, sleeper shape and properties of rail pads and ballast. It is concluded that the sound power generated by sleepers is influenced more by ballast stiffness and damping and by rail pad stiffness than by the sleeper design itself. Reductions in sound power can, however, be obtained by increasing sleeper mass and by reducing radiating sleeper area.

By adopting a bi-bloc design instead of a mono-bloc design, several advantages with respect to acoustic optimization can be obtained. The bending modes of the

two shorter concrete blocs are pushed towards higher frequencies where reduced vibration amplitudes are expected due to higher ballast stiffness [7]. Choosing a sufficiently weak connecting bar provides vibration isolation between the blocs. The radiating sleeper area is reduced. The centre section of the mono-bloc sleeper, which normally is supported by reduced stiffness due to ballast tamping, is omitted. In Figures 10 and 11, the influence of dimensions and length of the connecting bar on A-weighted sound power level is illustrated and compared with the data for the reference mono-bloc sleeper. Results are shown for roughness profiles corresponding to disc- and block-braked wheelsets [9]. The connecting bars are equilateral angle bars. Bloc dimensions are listed in the figure captions.

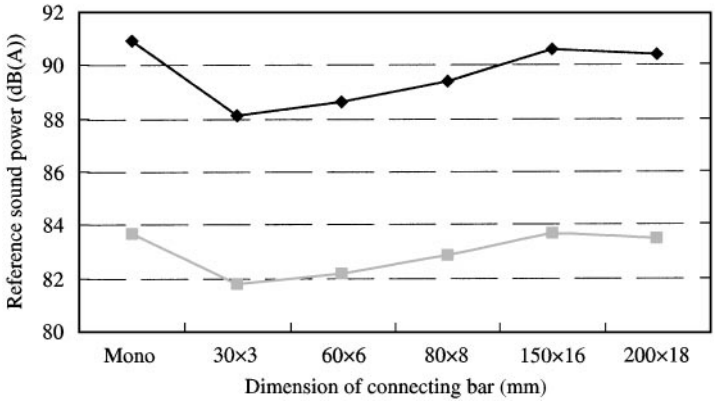

Figure 10. Reference sound power level (dB(A)) versus dimension of bi-bloc connecting bar. Connecting bars $x \times y$ are equilateral angle bars with width x mm and thickness y mm. Bi-bloc dimensions: $250 \times 225 \times 1000$ mm. Roughness spectrum corresponding to block- and disc-braked wheelset respectively. Ballast stiffness increasing linearly with frequency. —◆—, block; —■—, disc.

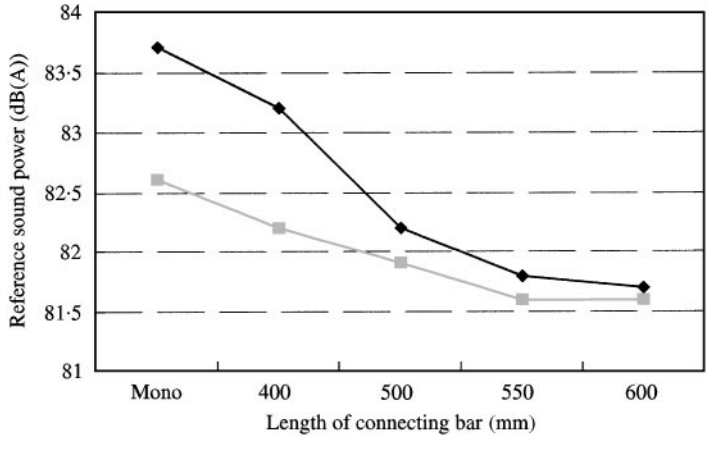

Figure 11. Reference sound power level [dB(A)] versus length of bi-bloc 60×6 connecting bar. Bi-bloc dimensions: 250×225 mm and symmetric with respect to railseat. Roughness spectrum corresponding to disc-braked wheelset. Symmetric and antisymmetric track vibration. Ballast stiffness increasing linearly with frequency. —◆—, symmetric; —■—, antisymmetric.

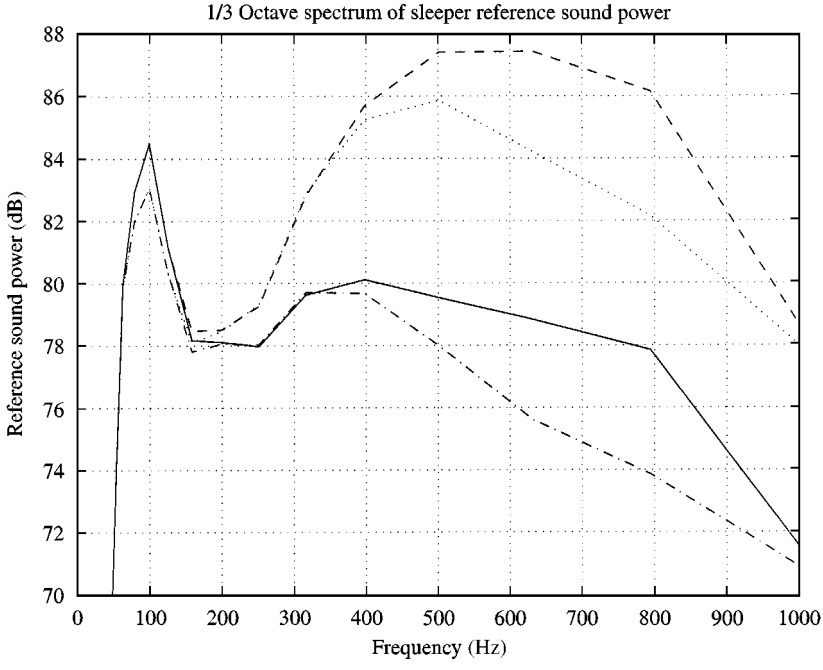

Figure 12. 1/3 octave band spectra of sleeper reference sound power. Mono-block and bi-bloc sleeper design. Roughness spectrum corresponding to block- and disc-braked wheelset respectively. Ballast stiffness increasing linearly with frequency. ———, mono-bloc disc 83·7 dB(A); – – –, mono-bloc block 90·9 dB(A); · – · – · –, bi-bloc disc 82·0 dB(A); · · · · · ·, bi-bloc block 88·7 dB(A).

In Figure 12, 1/3 octave band spectra of sleeper reference sound power are displayed for a bi-bloc sleeper with bloc dimensions $250 \times 200 \times 950$ mm. The connecting bar is a flat bar with dimensions 60×12 mm and length 600 mm. The corresponding spectra for a mono-bloc sleeper are shown for comparison. It is seen that a 2–3 dB (A) acoustic gain can be expected.

7. CONCLUDING REMARKS

The present study has dealt with the acoustic optimization of railway sleepers. A mathematical model for minimization of reference sound power generated by a single sleeper has been described. By use of the model, the influence of sleeper material properties, sleeper shape and properties of ballast and rail pads on sleeper sound power can be easily examined. The most important parameters determining the noise radiation from sleepers are rail pad stiffness and ballast properties. Low rail pad stiffness isolates the sleepers from the rails. A high ballast bed modulus reduces sleeper vibration amplitudes. Adopting a bi-bloc design will reduce sound power from the sleeper bending modes.

Boundary element simulations performed to compare mono-bloc and bi-bloc designs indicate that the influence of sleeper shape on radiation efficiency is negligible. Thus, the reference sound power levels obtained by use of the described mathematical wheelset/track interaction model can be directly adopted to judge the efficiency of different sleeper shapes.

Note that the present investigation has only focused on the acoustic optimization of railway sleepers. It was concluded that a bi-bloc sleeper with appropriate dimensions of the connecting bar and sufficient bloc mass can lead to a 2–3 dB (A) reduction of sound power. However, operational requirements on the sleeper such as production, assembly, handling, maintenance, cost and ability to maintain track gauge have not been addressed.

ACKNOWLEDGMENTS

Mr Tomas Fernström implemented the wheelset/track interaction model in a computer program. Mr Markus Wallentin performed the boundary element simulations. The present work was conducted as part of the Brite/EuRam III project Silent Track.

REFERENCES

1. D. J. Thompson 1998 *ISVR*, *Contract Report No.* 98/14, 9pp. An overview of results predicted from studies of rail shape and damping, pad stiffness and fastener design and new sleepers.
2. N. Vincent, P. Bouvet, D. J. Thompson and P. E. Gautier 1996 *Journal of Sound and Vibration* **193**, 161–171. Theoretical optimisation of track components to reduce rolling noise.
3. D. J. Thompson and M. H. A. Janssens 1997 *Report TPD-HAG-RPT*-93-0213. *TNO*, *Delft*, *The Netherlands*. TWINS: track-wheel interaction noise software user's manual version 2.4.
4. D. J. Thompson and M. H. A. Janssens 1997 *Report TPD-HAG-RPT*-93-0214, *TNO Dft*, *The Netherlands*, TWINS: track-wheel interaction noise software theoretical manual version 2.4.
5. T. Fernström 1997 *Thesis for the Degree of Master of Science*, *Report EX* 1997: 14. *Department of Solid Mechanics*, *Chalmers University of Technology*, *Gothenburg*, *Sweden*. Structural dynamics optimisation of railway sleepers.
6. S. Cox 1997 *Brite/EuRam III Silent Track*, *Document* 72105/3/*PAND*/*T*/*ReferenceTrack Proposal*2, *access restricted*. Reference track proposal—Version 2.
7. N. Frémion, J. P. Goudard and N. Vincent 1996 *Vibratec*, *Dardilly*, *France*, *Report* 072.028. Improvement of ballast and sleeper description in TWINS step 1: experimental characterisation of ballast properties.
8. K. Knothe and S. L. Grassie 1993 *Vehicle System Dynamics* **22**, 209–262. Modelling of railway track and vehicle/track interaction at high frequencies.
9. D. J. Thompson 1997 *Brite/EuRam III Silent Track*, *Document* 70128/3/*ISVR*/*T*/*A*/*stdrough.doc*, *access restricted*. Definition of the reference roughness.
10. L. Ågårdh 1990 *Report SP-AR* 1009-09, 43 pp. *Swedish National Testing Institute*, *Byggnadsteknik*, *Borås*, *Sweden*, Reinforced concrete sleepers—determination of resonance frequencies, modal dampings and modal shapes by use of experimental modal analysis (in Swedish).
11. J. O. C. Nielsen 1998 *Brite/EuRam III Silent Track*, *Document* 80801/3/*CHAL*/*T*/*A*1/*prel-sleepdesign*, *access restricted*. Parametric study on low noise sleeper design.
12. *LMS Numerical Technologies*, *Leuven*, *Belgium*. SYSNOISE rev 5.3 User's Manual.